*American Mineralogist, Volume 86, pages 1117–1129, 2001*

# Recalibration of the GASP geobarometer in light of recent garnet and plagioclase activity models and versions of the garnet-biotite geothermometer

**M.J. HOLDAWAY***

Department of Geological Sciences, Southern Methodist University, Dallas, Texas 75275, U.S.A.

## ABSTRACT

The garnet-Al silicate-plagioclase (GASP) geobarometer has been recalibrated using four recent garnet activity models, four analogous garnet-biotite temperature models, and two recent plagioclase activity models. A typical sillimanite-bearing sample that formed at about 5.25 kbar, 575 °C shows a possible *P* range of ~0.7 kbar due to *T* error, ~1 kbar due to range of garnet activity model, ~0.9 kbar due to range of plagioclase activity model, and ~5.4 kbar due to range of experimental end-member reversals extended by one sigma.

Calibrations were further constrained with the kyanite-sillimanite (K-S) phase boundary such that the best fit of 76 pelitic schist samples from 11 localities provides an individual end-member calibration for each of the eight possible combinations of garnet and plagioclase activity models with the appropriate geothermometer. Samples with low grossular or anorthite component were rejected. The end-member calibrations are constrained to pass through the the best-determined portion of the GASP experimental reversals at 1230 °C, 26.6 kbar. These individual end-member calibrations provide self-consistent models that tend to compensate for error in the garnet and plagioclase activity expressions. The models were also tested on a set of 59 samples from the Alps.

The recommended calibration is the average garnet activity model and average garnet-biotite *T* model of Holdaway (2000), the Fuhrman and Lindsley (1988) plagioclase activity model, and $H_{Grs}$ = –6628521, $S_{Grs}$ = 258.76 to combine with the remaining phases in the Berman database to produce the optimum end-member GASP curve. These thermodynamic data are for the GASP geobarometer only. Error is about ±0.8 kbar absolute and about ±0.6 kbar relative. Geological error is the largest component of error in many of these samples. Care should be taken to be sure that analyzed plagioclase and biotite are near analyzed garnet, that the peak-*T* portions of garnet and plagioclase are selected, that the peak-*T* Al silicate is determined, and that the *T* calculated is the most accurate possible. These calibrations represent an improvement over previous published GASP calibrations. These eight models are available for distribution as three programs (*T*, *P*, *P-T* intersection) for the DOS-based personal computer.

## INTRODUCTION

The garnet–Al-silicate–plagioclase (GASP) geobarometer is represented by the reaction

$$\underset{\text{Garnet}}{Ca_3Al_2Si_3O_{12}} + 2\ \underset{\text{Al-Silicate}}{Al_2SiO_5} + \underset{\text{Quartz}}{SiO_2} = 3\ \underset{\text{Plagioclase}}{CaAl_2Si_2O_8} \quad (1)$$

with grossular component in garnet and anorthite component in plagioclase having variable activity. GASP was first proposed by Ghent (1976) and has been widely used. It has been nearly a decade since anyone has rigorously investigated the GASP geobarometer and during that time three new garnet activity models have been proposed (Berman and Aranovich 1996; Ganguly et al. 1996; Mukhopadhyay et al. 1997) and two plagioclase activity models are now available (Fuhrman and Lindsley 1988; Elkins and Grove 1990). Most GASP calibrations after 1988 (e.g., Berman 1988, revised 1992) have been done with the Fuhrman and Lindsley model. One might suppose that each new garnet or plagioclase activity model could simply be applied to the existing end-member experimental data to upgrade the geobarometer, but these recent activity models still allow for a range of *P* values (see below).

Two differing approaches to geothermobarometric calibration have been used: (1) a geothermometer or geobarometer is independently calibrated using available primary experimental data. Primary data are defined as those involving only the phases and reactions present in reaction 1, whereas secondary data involve additional reactions and phases. Such an approach was used by Holdaway et al. (1997) and Holdaway (2000) for the garnet-biotite geothermometer. (2) A self-consistent thermodynamic database is developed using statistical or mathematical programming methods applied to all the experimental data available for numerous related compositional systems. Such a self-consistent model is that of Berman (1988, revised 1992). The former approach has the value that because only the primary constraints are considered, and the result is not

* Present address: 855 Elliott St., Longmont, CO 80501. E-mail: holdaway@mail.smu.edu

0003-004X/01/0010–1117$05.00

biased by secondary constraints, better accuracy may potentially be achieved. The latter approach has the value that using a database, numerous equilibria may be applied to a given specimen to solve a *P-T* problem, and thus one may be able to determine whether equilibrium has been achieved, or perhaps more tightly constrain the *P* and *T*. However, if secondary constraints involve systematic errors in thermodynamic data and related *P-T* equilibria, it is quite possible that the latter approach may have systematic *P* and *T* errors between specimens of differing compositions, between differing *P* and *T* conditions of formation, or between various equilibria. Because of this, error may still be larger than for a carefully calibrated individual geothermobarometer. Ultimately, some of the well-calibrated individual geothermobarometers may serve as constraints, within error, for the thermodynamic database. Thus both approaches are important. I have chosen the individual calibration approach for this work on the GASP equilibrium.

## THE GASP FORMULATION

The pressure equation for GASP is as follows:

$$P\,(\text{bar}) = \frac{\Delta H - T\Delta S}{-\Delta V} + \frac{RT\ln K_{Eq}}{-\Delta V} + \frac{RT\ln K_{\gamma}}{-\Delta V} + 1.0. \qquad (2)$$

where $\Delta H - T\Delta S$ is the standard Gibbs energy and $\Delta V$ is the molar volume change of the kyanite or sillimanite GASP end-member reaction 1, $K_{Eq}$ is the ratio of anorthite mole fraction to grossular mole fraction, each cubed, and $K\gamma$ is the ratio of anorthite activity coefficient to grossular activity coefficient, each cubed. Molar volume of reaction 1 is integrated at *T* from 1.0 bar to *P*, and $K\gamma$ is determined at *P* and *T*. The equation can be thought of as having two parts, the end-member *P* based on the first and last term with $K_D = K\gamma = 1.0$ for the second and third terms, and the *P* change that results from dilution of grossular and anorthite by other components, given as the second and third terms. Temperature must be determined independently, e.g., using the garnet-biotite geothermometer.

## SOME PREVIOUS CALIBRATIONS OF GASP

Two of the more widely cited calibrations of GASP, which involve determination of both *T* and *P,* are those of Hodges and Spear (1982) and Berman (1988, revised 1992, 1990). The Hodges and Spear (GASPHS) calibration predates the Koziol and Newton (1988) end-member calibration and the recent garnet and plagioclase activity models. It uses a local charge balance plagioclase activity model with an activity coefficient of 2.0. This calibration is still in use (e.g., Spear et al. 1995). The Berman calibration (GASPB92) includes the Koziol and Newton data and is based on the Berman database (1988, revised 1992), the garnet activity model of Berman (1990), the garnet-biotite geothermometer of McMullin et al. (1991), and the plagioclase activity model of Furhman and Lindsley (1988). Rob Berman (personal communication, 2000) is presently working on an improved self-consistent GASP geobarometer and garnet-biotite geothermometer that should be a substantial improvement over this earlier version. These two calibrations (GASPHS and GASPB92) were tested in addition to eight new calibrations. End-member GASP curves for these previous models are shown in Figure 1a relative to the experimental data for reaction 1 extended to their one sigma limits away from the equilibrium curve (see below).

## PERMITTED PRESSURE RANGES FOR GASP

For the following discussion and throughout this report, I have used the Berman (1988, revised 1992) model for all GASP end-member thermochemical data except for *H* and *S* of grossular, which are kept as adjustable parameters, within limits. This in no way implies that all possible error in the Berman database lies in the grossular, but implies only that it is necessary to allow for a range of $\Delta H$ and $\Delta S$ of reaction 1 in testing various possibilities, and this is a convenient way to do it. It also underscores the fact that there are still substantial errors in the available thermodynamic databases. Any other phase (e.g., anorthite) participating in the reaction could have been picked as the variable to allow for alternative possible values of $\Delta H$ and $\Delta S$ of the GASP equilibrium.

The plots in Figure 1 are $\Delta P$-*T* plots, and $\Delta P$ is the difference between the experimental data points and the York-type linear least-squares fit by McKenna and Hodges (1988) of the experimental reversals for reaction 1. For each plot the horizontal line at zero $\Delta P$ is the McKenna and Hodges fit. The GASP experimental data of Hays (1966), Hariya and Kennedy (1968), Goldsmith (1980), Gasparic (1984), and Koziol and Newton (1988) have been shown by McKenna and Hodges to be a self-consistent set. In these plots of Figure 1, each experimental reversal is represented by two points, one on each side of the equilibrium curve, each extended away from the equilibrium curve by estimated one sigma values of *P* and *T*. A half-reversal is shown as a single point. Estimated 1σ values are 5 °C, 0.54 kbar for Koziol and Newton (1988), 5 °C, 0.5 kbar for Gasparic (1984), and 10 °C, 1.0 kbar for the other three studies. A similar approach was used by Holdaway and Mukhopadhyay (1993).

Three primary constraints are needed for a geobarometer such as GASP: (1) a way to determine *T* and estimate its error; (2) activity models for each of the participating phases having variable composition; and (3) an end-member reaction calibration. The three garnet and two plagioclase activity models cited above are the best available at present [see Holdaway 2000, regarding the garnet models]. The most optimistic estimate of error in *T* determination is about ±25 °C (Holdaway 2000).

The extended reversals of Figure 1 provide for end-member constraints. Contrary to McKenna and Hodges (1988), I believe that the York-type regression of the experimental data does not provide a significantly more probable end-member calibration than any other line drawn between the extended experimental reversals. Because of the likelihood of systematic errors in the experimental data, any curve that passes between the closed and open squares of Figure 1 has similar probability of being the correct end-member curve. These likely systematic errors include: (1) the fact that dense high-*P* phases tend to nucleate and grow more slowly than less dense low-*P* phases, and this phenomenon is exaggerated at lower *T* where kinetic factors prevail; and (2) friction corrections may be too low, or may need to be increased at lower values of *T*. These likely systematic errors may explain why the existing end-member calibrations (Fig. 1a) pass through the lower part of the

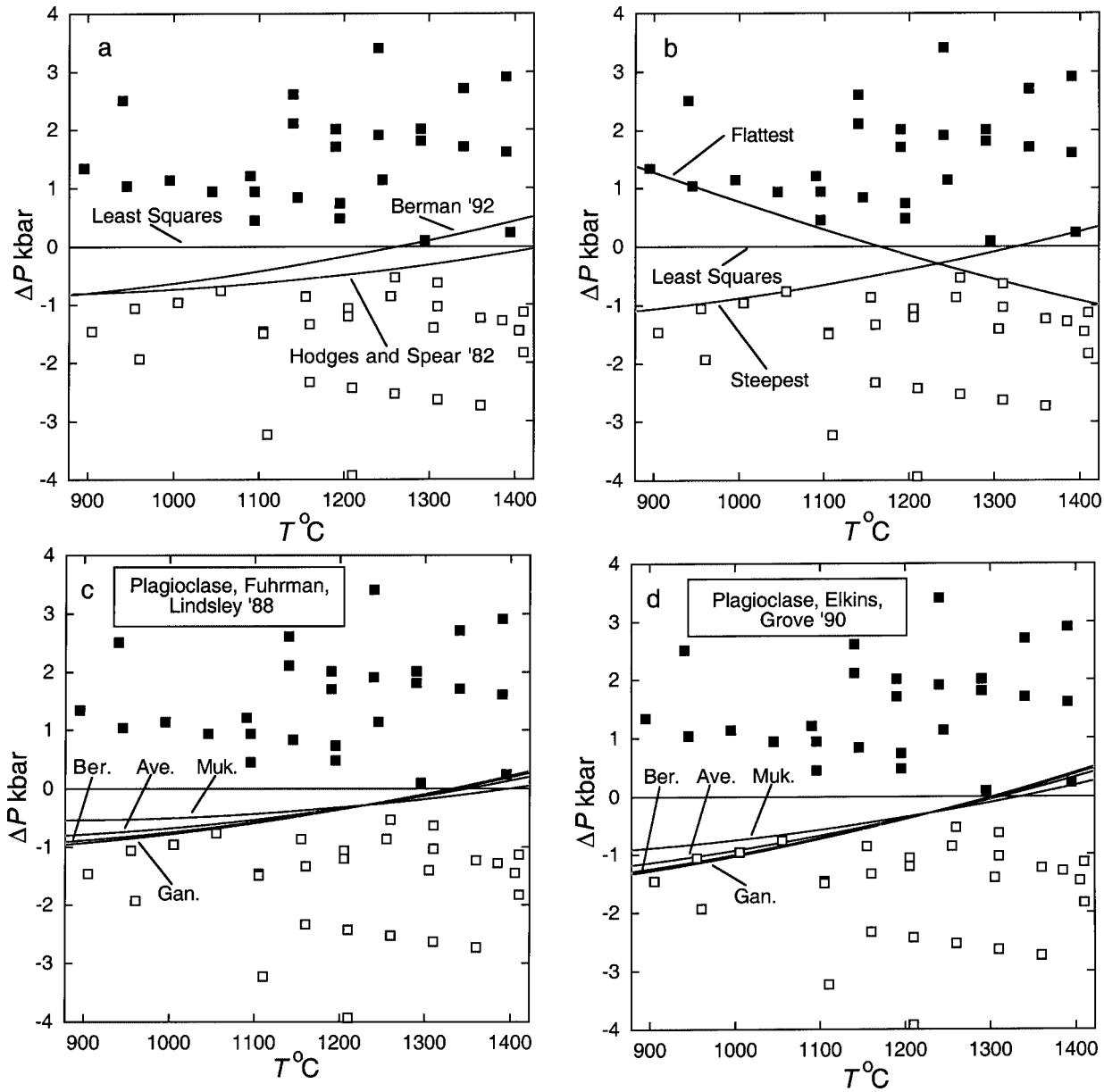


**FIGURE 1.** Plots of $\Delta P$ vs. $T$ of end-member data for GASP, reaction 1, designed for maximum amplification. $\Delta P$ is the $P$ difference between the McKenna and Hodges (1988) linear least-squares line, $P$ (kbar) = 0.022$T$ (K) – 6.2, and experimental or calculated end-member $P$ data. Squares are GASP reversal data extended one sigma away from the equilibrium curve: closed = grossular + kyanite + quartz stable, open = anorthite stable. Except for the horizontal least-squares line, lines are calculated from the Berman (1988, revised 1992) database with $H_{Grs}$ and $S_{Grs}$ allowed to vary to fit the situation as explained in the text. (**a**) GASP end-member curves for the Hodges and Spear (1982) and Berman (1988, revised 1992) calibrations. (**b**) Flattest possible end-member GASP equilibrium ($H_{Grs}$ = –6571375 J/mol, $S_{Grs}$ = 296.80 J/K mol) and steepest ($H_{Grs}$ = –6635840 J/mol, $S_{Grs}$ = 253.97 J/K mol) consistent with extended reversals. (**c**) GASP end-member curves based on this report using the Fuhrman and Lindsley (1988) plagioclase activity model. Garnet activity models are Ber. = Berman and Aranovich (1996), Gan. = Ganguly et al. (1996), Muk. = Mukhopadhyay et al. (1997) and Ave. = average of these three. (**d**) GASP end-member curves based on this report using the Elkins and Grove (1990) plagioclase activity model and the same garnet models as given for (c).

field between the extended reversals. For this work, I assume that systematic errors allow for similar probability within the 1-σ extended field, but that the probability of the equilibrium curve violating reversals by more than 1-σ decreases away from the equilibrium curve. Thus, I have chosen the range from the highest d$P$/d$T$ (steepest) to the lowest d$P$/d$T$ (flattest) curve that violate none of the extended reversals (Fig. 1b) as the likely range for the end-member equilibrium based on experimental constraints. There is an additive component to $P$ error estimation in the $T$ range of the experiments (Hodges and McKenna 1987), but the slope error is the only significant factor in the geological range of $T$ (McKenna and Hodges 1988, Fig. 1b).

If the errors of all the other parts of the determination (analytical, geological, molar volume) are neglected, it is possible to show the range of $P$ values that can be calculated on the basis of the permissible range for each of the three above primary constraints. In this exercise, we make the reasonable assumption that the range of garnet activity models and the range of plagioclase activity models give rough indications of the errors of these models. Table 1 illustrates the range of $P$ values possible for a single representative sillimanite-bearing (kyanite-absent) sample that contains garnet with 7.4% grossular and plagioclase with 31% anorthite, and that crystallized at about 575 °C and 5.25 kbar (based on the results of this report), lying on or near the kyanite-sillimanite (K-S) boundary. The calculated $P$ values range from 3.50 to 11.38 kbar (~8 kbar range). The variation due to the range of $\Delta H$ and $\Delta S$ permitted by the extended end-member constraints (Table 1, Fig. 1b) is between 5.17 and 5.60 kbar depending on $T$. Variation due to $T$ error of ±25 °C is between 0.31 and 1.03 kbar. That due to the garnet activity model is between 0.89 and 1.05 kbar. That due to the plagioclase activity model is between 0.77 and 1.00 kbar.

The important conclusions to be drawn from this experiment are: (1) the range of possible $P$ solutions allowed by the primary data is too large for the GASP geobarometer to be useful in this form; (2) despite the fact that the GASP end-member equilibrium is one of the best-calibrated geobarometers (McKenna and Hodges 1988), the end-member calibration represents the greatest contribution to $P$ error of these factors; and (3) for any satisfactory calibration, the end-member curve must be adjusted, within limits, to be consistent with the particular geothermometer and garnet and plagioclase activity models being used.

This last important point illustrates the fact that unless the end-member curve is known precisely, one cannot simply add a new garnet or plagioclase activity model to an existing end-member calibration of GASP and obtain a satisfactory result. Alternatively, if one accepts a particular database for the end-member equilibrium, then the garnet and plagioclase models and $T$ calibration must be made consistent with that database, an exercise that is becoming increasingly more difficult as the quality of these $T$ determinations and activity models improves (Holdaway 2000). Adjustment of the end-member curve tends to correct for systematic error in the experiments on which the end-member curve is based and to compensate for error in the garnet and plagioclase activity models and $T$ calibration over a range of composition and $P$-$T$ conditions. If I knew the end-member curve precisely, I could then make appropriate adjustments to the $T$ model and activity models, but I do not, and in fact, I am simply trying to arrive at the best possible consistent calibration that minimizes the errors in all the constraints. Given the fact that the possible $P$ range from end-member equilibrium is about five times as large as that from garnet, plagioclase, or $T$ models, it is not appropriate, in my opinion, to adjust the activity models and/or $T$ determination to fit the least-squares line through the extended reversals of the end-member reaction.

**TABLE 1.** $P$ range (kbar) for sample 2-13 due to range in end-member calibration, plagioclase activity model, garnet activity model, and $T$ error of ±25 °C.

| Plagioclase Model | Fuhrman and Lindsley 1988 | | Elkins and Grove 1990 | |
|---|---|---|---|---|
| $T$ °C | 550 | 600 | 550 | 600 |
| Muk-F | 9.07 | 9.71 | 10.05 | 10.49 |
| Ber-F | 10.10 | 10.62 | 11.10 | 11.41 |
| Gan-F | 10.07 | 10.60 | 11.06 | 11.38 |
| Muk-S | 3.50 | 4.53 | 4.47 | 5.31 |
| Ber-S | 4.52 | 5.43 | 5.50 | 6.21 |
| Gan-S | 4.49 | 5.41 | 5.46 | 6.18 |

*Notes*: Sample is a representative sillimanite-bearing specimen from Azure Lake (Pigage 1982). Garnet activity models: Muk = Mukhopadhyay et al. (1997), Ber = Berman and Aranovich (1996), Gan = Ganguly et al. (1996). F = flattest possible end-member equilibrium ($H_{Grs}$ = –6571375, $S_{Grs}$ = 296.80), S = steepest ($H_{Grs}$ = –6635840, $S_{Grs}$ = 253.97), see Figure 1b and text.

At the present time there are only two ways to further constrain GASP. The first is to include additional secondary constraints to further limit the end-member equilibrium, such as other equilibria involving the Ca-Al silicates (i.e., the database approach). However, with this approach, each secondary constraint that is added produces one or more additional sources of error for each of the secondary constraints. For example, adding hydrous equilibria adds error from the thermodynamic properties of water, which are potentially large in the $P$-$T$ range of the GASP end-member curve. In addition, such an approach does not address the differences in $P$ among recent garnet and plagioclase activity models and $T$ calibrations if a specific end-member calibration is adopted (Table 1). The second approach is to use a well-determined $P$-$T$ equilibrium to constrain the GASP system on the basis of natural occurrences and allow the GASP end-member equilibrium to vary within limits, reflecting the error of the original end-member experiments and the garnet, plagioclase, and $T$ models. The obvious candidate is the K-S phase boundary, because it is reasonably accurately determined, and more importantly, because the Al silicates are involved in the GASP equilibrium. Difficulties can arise if the GASP and Al-silicate equilibria are inconsistent. For example, should a sillimanite-bearing rock that plots in the kyanite field have its $P$ calculated according to the sillimanite or the kyanite version of reaction 1?

There are also problems associated with calibration using natural samples. Geological and analytical error can compound to produce substantial discrepancies in some samples. Important parts of the geological error include the choice of grains and parts of grains for analysis, and the decision regarding which Al-silicate was stable at peak $T$. These points will be discussed in more detail below. In calibrating with natural specimens it is important to use a large number of specimens and localities in an effort to average out these effects. One must also avoid putting too much emphasis on any one sample because of the error sources mentioned above.

In this contribution, I use the four garnet-biotite geothermometers proposed by Holdaway (2000), the extended end-member constraints of the GASP equilibrium, the three recent garnet activity models and an average of these three, the two plagioclase activity models, and the K-S phase boundary to constrain the geobarometer as it is applied to naturally occurring GASP assemblages of 76 pelitic schists from 11 localities to provide eight calibrations of the GASP geobarometer. These calibrations are tested on 59 samples from the Lepontine Alps. The eight models tested are designated GASPGF,

GASPMF, GASPBF, GASPAF, GASPGE, GASPME, GASPBE, and GASPAE. The fifth letter designates the garnet model (G = Ganguly et al. 1996; M = Mukhopadhyay et al. 1997; B = Berman and Aranovich 1996; A = average of these three) and the analogous version of the garnet-biotite geothermometer (Holdaway 2000). The Mn interactions for all the garnet models are those of Ganguly et al. (1996), as modified by Holdaway (2000) by adding 5 kJ to the enthalpy term. The sixth letter refers to the plagioclase model (F = Fuhrman and Lindsley 1988, E = Elkins and Grove 1990).

## PROCEDURE

A program was written to duplicate the calculations of the Berman (1988) Ge0calc program for reaction 1 using Equation 2. This program includes integration of $C_P$ to evaluate enthalpy and entropy at $T$, evaluation of molar volume at $T$, integration of molar volume over $P$, the alpha-beta quartz transition, and calculation of garnet and plagioclase activity from chemical and Margules data. For garnet, the Margules equations of Mukhopadhyay et al. (1993) were used, and for plagioclase the Margules equations of the authors (Fuhrman and Lindsley 1988, or Elkins and Grove 1990) were used. As with the garnet-biotite geothermometer (Holdaway 2000), $Fe^{3+}$ content of garnet was assumed to be 3% of total Fe. Results were tested against Ge0calc and match precisely. Data files include one batch file for $T$, specimen analytical data of plagioclase and garnet, and whether the rock contains kyanite, sillimanite, or andalusite; and one for garnet and plagioclase Margules data along with $H_{Grs}$ and $S_{Grs}$. The program asks whether to base the calculations on alpha or beta quartz. It was designed so that a variable, $\Delta S_{Grs}$, could be used to vary $H_{Grs}$ and $S_{Grs}$ in such a way that the end-member curve for GASP was rotated about a "fulcrum" at 1230 °C, 26.6 kbar. This corresponds to the intersection of the steepest and flattest possible end-member curves (Fig. 1b) and is the best-constrained part of the experimental GASP end-member curve. Any further allowance for error at this high $P$ and $T$ does not provide for any increased accuracy of the final results for geologic conditions.

Naturally occurring typical $Fe^{2+}$-rich pelitic schists from 11 localities (Table 2) were used to calibrate GASP for each of the four garnet activity models, four geothermometers and two plagioclase activity models. Samples from two localities contained andalusite. For Augusta, Maine, Ferry (1980) studied several samples with andalusite and no sillimanite. These andalusite-bearing samples have been interpreted as polymetamorphic, with andalusite resulting from the earlier (M2) event (Novak and Holdaway 1981; Holdaway et al. 1982, 1988). At Mt. Moosilauke, New Hampshire, Hodges and Spear (1982) analyzed two andalusite-bearing samples that also contain sillimanite. For the present study, andalusite-bearing samples were omitted unless they also contained sillimanite, and such rocks were then designated as sillimanite-bearing. Where both kyanite and sillimanite occurred in a sample, sillimanite, the higher-$T$ mineral was designated as stable when it occurred in more than trace amounts. Thus, the few tiny needles of sillimanite found by Lang (1991) in some of the kyanite-bearing rocks at Hunt Valley Mall were ignored whereas 0.5–1% (or more) of sillimanite in many other samples was considered to indicate peak-$T$ conditions. The possibility exists that the $P$-$T$ path experienced by some samples was steep enough that kyanite formed from sillimanite with increasing $T$. This possibility is discussed below. Rim garnet and plagioclase compositions were used unless a $T$ determination showed the measured garnet rim to be significantly retrograded, in which case a core or inner rim (if available) was chosen.

In a GASP $P$-$T$ plot for any calibration for a particular locality, it was seen that there was a considerable scatter of data resulting in part from the use of samples with very low grossular in garnet and/or anorthite in plagioclase (Todd 1998). This scatter results from increased relative analytical error for samples containing small amounts of Ca. For this study, an effort was made to be as conservative as possible in rejecting samples with low Grs and/or low An, to avoid favoring any particular activity model. Samples with low grossular and anorthite content were successively deleted until the composition was reached above which low-Grs and low-An $P$ outliers for any given locality were eliminated. For three papers prior to 1980, all samples with Grs < 4 and/or An < 22 were omitted, and for eight papers from 1980 to 1995, all samples with Grs < 3 and/or An < 17 were omitted. These deleterious dilution effects are believed to be partly due to analytical error and partly due to error in the garnet and plagioclase activity models. The larger limits for rejection in plagioclase probably result from the fact that the activity models do not adequately reflect anorthite activity near the peristerite solvus.

In addition to samples rejected because of low grossular or

**TABLE 2.** Localities, references and percentage composition range of samples used for GASP calibration and verification

| Locality | Reference | No. Kya | No. Sil | Grs Range | An Range |
|---|---|---|---|---|---|
| Hunt Valley Mall, MD, U.S.A. | Lang (1991) | 6 | 0 | 5–7 | 20–29 |
| Mt. Moosilauke, NH, U.S.A. | Hodges and Spear (1982) | 0 | 3 | 4–6 | 24–27 |
| Azure Lake, BC, Canada | Pigage (1982) | 3 | 9 | 4–10 | 20–39 |
| Augusta, ME, U.S.A. | Ferry (1980) | 0 | 6 | 3–7 | 22–47 |
| West-Central ME, U.S.A. | Holdaway et al. (1988) | 0 | 10 | 3–7 | 18–53 |
| Quabbin Reservoir, MA, U.S.A. | Tracy (1975) | 0 | 5 | 4–5 | 27–40 |
| Grampian Highlands, Scotland | McLellan (1985) | 5 | 3 | 5–13 | 18–32 |
| Snow Peak, ID, U.S.A. | Lang and Rice (1985a, b) | 6 | 0 | 5–11 | 17–33 |
| West-Central NH, U.S.A. | Spear et al. (1995) | 0 | 8 | 3–8 | 21–39 |
| Yale, BC, Canada | Pigage (1976) | 4 | 2 | 7–14 | 28–34 |
| Penfold Cr., BC, Canada | Fletcher and Greenwood (1979) | 1 | 5 | 4–9 | 26–36 |
| Totals | | 25 | 51 | 3–14 | 17–53 |
| Lepontine Alps, Switzerland | Engi et al. (1995)*; Todd, Engi (1997)* | 46 | 13 | 3–23 | 17–74 |

*And references therein.

anorthite and andalusite without sillimanite, three samples from the Grampian Highlands (McLellan 1985) were rejected (not plotted or used for calibration) because they contain sillimanite but plot in the kyanite field by 1 to 3.5 kbar by all eight calibrations. These samples will be discussed below. There remained 76 samples, 25 with kyanite as the peak-*T* mineral and 51 with sillimanite.

Temperature was calculated using the four garnet-biotite calibrations of Holdaway (2000). Pressure was calculated using Equation 2. The variable $\Delta S_{Grs}$ (see above) allows for optimization of the separation between kyanite- and sillimanite-bearing samples into the appropriate *P-T* fields by varying GASP end-member Gibbs energy about the fulcrum. A separate program does a linear solution of two GASP *P-T* points and two garnet-biotite *P-T* points to calculate a unique *P* and *T* for each sample. Error resulting from the linear approximation varies between 0.001 and 0.01 kbar. The error can be reduced to 0.001 kbar by entering the initial *P* and *T* results into the original data file and repeating the calculations.

The final step in the optimization process was to separately average *T* and *P* of all 76 samples for each of the eight new calibrations and make further slight adjustments of $H_{Grs}$ and $S_{Grs}$ about the fulcrum to have the average *P* and *T* of all eight calibrations fall on *P-T* lines with a slope of 19 bar/deg for the Fuhrman and Lindsley (1988) plagioclase activity model and 17 bar/deg for the Elkins and Grove (1990) plagioclase activity model, the approximate slopes of the GASP equilibrium near the center of the *P-T* field. This procedure brings each set of four calibrations into maximum consistency with the other three.

## Results

The results of these calibrations for the eight models are shown and compared to the two previous calibrations in Figures 1a, 1c, and 1d for end-member curves and Table 3[1] and Figure 2a–d (for representative calibrations) showing calculated values of *P* and *T* for the natural specimens. For maximum clarity, Figure 2 is drawn so as to include all the *P-T* values of the samples used for the new calibrations. All four fields (Figs. 2a–2d) are the same *P-T* size for ease in comparison. Points in Figures 2a and 2b that fall outside the field are indicated by italicized numbers at edges or corners of the plot and are listed in the caption. On these figures an overlap range is defined by two dashed lines parallel to the K-S boundary as calculated from the Berman (1988, revised 1992) database and linearized over the *P-T* range of interest. This overlap range includes all sillimanite data points that plot in the kyanite field and all kyanite data points that plot in the sillimanite field. Because there are twice as many sillimanite-bearing samples as kyanite-bearing samples, there are about twice as many sillimanite points in the kyanite field as kyanite points in the sillimanite field.

Table 4 provides semiquantitative data that serve for comparison of the ten calibrations in terms of how well they fit with the extended experimental end-member reversals and how well they discriminate between kyanite- and sillimanite-bearing rocks. The number in violation of the K-S boundary greater than 0.15 kbar is also given. The value of 0.15 kbar was chosen because the concentration of violating points begins to decrease at this degree of misfit. The slightly larger overlap range for the Hodges and Spear (1982) calibration than for the other nine (Table 4, Fig. 2b) suggests that it does not discriminate between kyanite- and sillimanite-bearing samples as well as the others. It also has a larger number of samples that violate the K-S boundary by more than 0.15 kbar. The remaining nine calibrations show smaller differences in fit with the K-S curve.

Table 5 gives the average and standard deviation of *P* and *T* for each of the localities for the four calibrations represented in Figure 2. As a measure of how small the calculated range of *P* can be for a localized area, consider the Hunt Valley Mall samples (Lang 1991). Six samples are distributed over 500 m in length. Using GASPAF, *P* values are 5.85 ± 0.39 (1σ) kbar. However, the three samples that occur over 200 m near the middle of the outcrop have *P* = 6.20 ± 0.11 kbar whereas the three outside samples have *P* = 5.50 ± 0.05 kbar, suggesting two prevalent pressures, perhaps the result of an anticlinal flexure or block faulting after the rocks reached peak *T* and were cooling down. The other seven calibrations show these same tendencies for this locality (Table 3).

An additional important point of comparison concerns the effect of *T* on the calculated *P*. Because the slope of the GASP end-member curve is similar to that of the K-S boundary (22 bars/° for K-S, ~17–19 bars/° for GASP), the *T* effect on *P* error does not show up on Figure 2 or in Table 4. As a result of the *P-T* slope of the GASP curve, the quality of *T* measurements translates directly into the quality of *P* measurements using GASP (Table 1). Thus an evaluation of the accuracy of the *T* values is necessary.

All but the highest-*T* sample (933B, 714 °C, GASPAF) from Quabbin Reservoir (Tracy 1975), contain the assemblage Al-silicate–biotite–garnet–muscovite–plagioclase–quartz ± staurolite. A very few have K-feldspar or chlorite in addition. Sample 933B is a migmatitic sample that contains no muscovite. Thus 75 of the 76 samples must lie between or on the reactions:

$$\text{Staurolite} + \text{Muscovite} + \text{Chlorite} = \text{Biotite} + \text{Al-silicate} + H_2O \quad (3)$$

and

$$\text{Muscovite} + \text{Plagioclase} = \text{K feldspar} + \text{Al-silicate} + H_2O \quad (4)$$

with excess quartz. Bulk compositions of most pelitic schists are such that the assemblage biotite–Al-silicate does not form until the staurolite composition field begins to shrink at slightly higher *T* than reaction 3, as garnet joins the assemblage. However it is more difficult to apply the terminal reaction for staurolite breakdown because of the stabilization of garnet-bearing assemblages to lower *T* by Mn and Ca. Excluding sample 933B,

[1]For a copy of Table 3, document item AM-01-070, contact the Business Office of the Mineralogical Society of America (see inside front cover of recent issue) for price information. Deposit items may also be available on the American Mineralogist web site (http://www.minsocam.org or current web address).

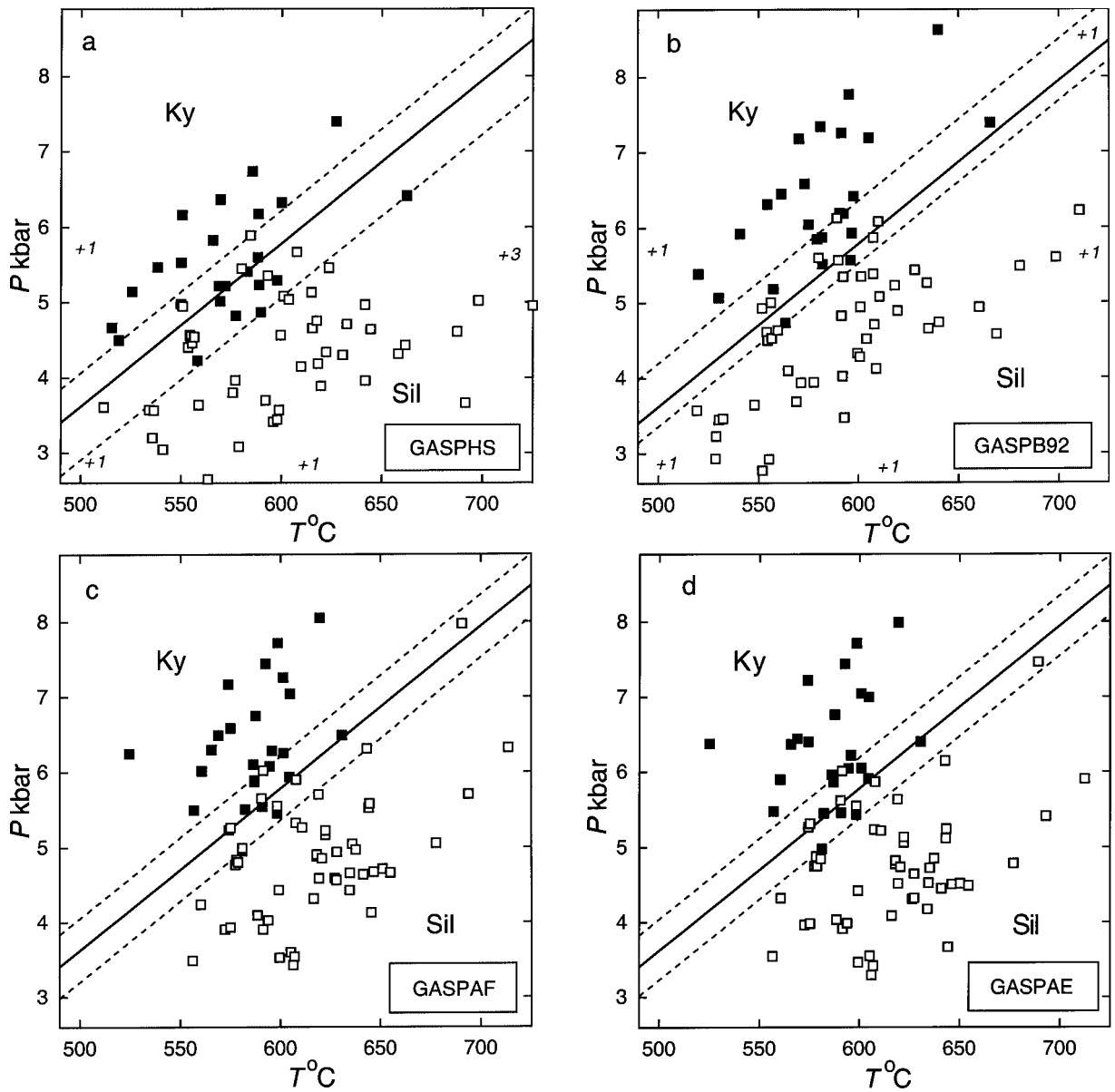


**FIGURE 2.** Calculated *P* and *T* for 76 samples from the 11 localities given in Table 2 (three additional samples were rejected as explained in text). Closed squares are samples that contain kyanite as the peak-*T* mineral, and open squares are samples that contain sillimanite. Solid line is the K-S boundary and dashed lines parallel to the K-S boundary delimit the fields of overlap, as explained in text. For ease of comparison, all plots occupy the same limited *P-T* field and, for **a** and **b**, the italicized figures give numbers of points plotting outside the field in that direction. (**a**) Hodges and Spear (1982) calibration (GASPHS). (*P-T* points outside the field include K = 4.67, 461; and S = 2.44, 477; 2.56, 566; 7.41, 868; 5.68, 751; 8.97, 813). (**b**) Berman (1988, revised 1992) calibration (GASPB92). (*P-T* points outside the field include K = 5.33, 478; and S = 2.17, 473; 2.58, 542; 8.26, 815; 10.03, 787). (**c**) This report, Fuhrman and Lindsley (1988) plagioclase activity model, average garnet activity model and Holdaway (2000) geothermometer based on average garnet model (GASPAF). (**d**) This report, Elkins and Grove (1990) plagioclase activity model, average garnet activity model and Holdaway (2000) geothermometer based on average garnet model (GASPAE).

the Hodges and Spear (GASPHS) calibration yields a range of *T* from 461 to 814 °C, and the Berman (GASPB92) calibration yields a range of *T* from 473 to 787 °C. Several of the lowest and highest *T* values for each of these calibrations lie outside the experimental range of the above assemblage, as shown below. On the other hand, the remaining calibrations yield the following ranges of *T* for the Fuhrman and Lindsley (1988) plagioclase model: GASPGF = 529–699 °C, GASPMF = 544–698 °C, GASPBF = 501–692 °C, GASPAF = 524–696 °C. Temperatures are nearly identical with the Elkins and Grove (1990) plagioclase model (GASPGE, etc.) because they were based on the same four geothermometers.

Spear (1993) showed the position of reaction 3 at about 600 °C at appropriate *P*. The effects of limited dilution of the $H_2O$-

**TABLE 4.** Comparison of two previous GASP calibrations and eight present calibrations

| Model | End-Member | | Maximum End-member Violation, Fig. 1b-d (kbar) | Overlap Range (kbar) | Midpoint Relative to K-S* (kbar) | No. in Violation > 0.15 kbar |
|---|---|---|---|---|---|---|
| | $S_{Grs}$ [J/(K mol)] | $H_{Grs}$ (J/mol) | | | | |
| GASPHS | 261.18† | –6625810† | 0.00 | 1.16 | –0.14 | 10 |
| GASPB92 | 255.15 | –6632859 | 0.18 | 0.84 | +0.16 | 5 |
| GASPGF | 256.07 | –6632566 | 0.00 | 0.87 | –0.01 | 4 |
| GASPMF | 263.35 | –6621621 | 0.00 | 0.85 | –0.06 | 4 |
| GASPBF | 256.89 | –6631332 | 0.00 | 0.84 | +0.09 | 4 |
| GASPAF | 258.76 | –6628521 | 0.00 | 0.85 | 0.00 | 4 |
| GASPGE | 249.50 | –6642441 | 0.15 | 0.83 | –0.01 | 3 |
| GASPME | 256.80 | –6631470 | 0.00 | 0.81 | –0.06 | 4 |
| GASPBE | 250.19 | –6641408 | 0.13 | 0.81 | +0.12 | 4 |
| GASPAE | 252.15 | –6638460 | 0.07 | 0.81 | 0.01 | 3 |

*Note:* Data based on 76 natural samples, Figures 1a,c,d, 2a–d Table 3 (Footnote 1). Models and explanation given in text.
* Midpoint of overlap range relative to the kyanite-sillimanite line.
† Values calculated using the Berman (1988, revised 1992) data base to reproduce the Hodges and Spear (1982) GASP end-member line.

**TABLE 5.** Temperature and pressure average and σ values (in parentheses) for the 12 localities based on the GASPHS, GASPB92, GASPAF, and GASPAE models

| Locality* | GASPHS | | GASPB92 | | GASPAF | | GASPAE | |
|---|---|---|---|---|---|---|---|---|
| | *T* (°C) | *P* (kbar) | *T* (°C) | *P* (kbar) | *T* (°C) | *P* (kbar) | *T* (°C) | *P* (kbar) |
| Hunt Valley Mall | 580(14) | 5.08(39) | 586(15) | 5.84(49) | 594(7) | 5.85(39) | 594(7) | 5.78(37) |
| Mt. Moosilauke | 508(29) | 3.16(60) | 507(30) | 2.99(73) | 568(18) | 3.94(40) | 568(17) | 3.97(39) |
| Azure Lake | 566(18) | 5.00(54) | 570(18) | 5.20(65) | 584(9) | 5.35(49) | 584(9) | 5.34(49) |
| Augusta | 571(23) | 3.22(47) | 555(22) | 3.27(59) | 608(13) | 4.03(48) | 608(13) | 3.91(47) |
| West-Central ME | 635(30) | 4.45(40) | 617(25) | 4.75(41) | 633(11) | 4.91(51) | 633(11) | 4.71(57) |
| Quabben Res. | 722(105) | 5.22(1.58) | 688(94) | 5.59(1.94) | 669(42) | 5.07(1.04) | 668(41) | 4.83(90) |
| Grampian High. | 600(105) | 6.05(1.53) | 603(93) | 6.80(1.80) | 600(49) | 6.61(1.19) | 599(49) | 6.50(1.14) |
| Snow Peak | 545(21) | 5.37(61) | 557(20) | 6.19(74) | 574(13) | 6.40(64) | 574(13) | 6.35(65) |
| West-Central NH | 612(20) | 4.28(64) | 599(19) | 4.56(77) | 629(15) | 4.93(80) | 628(14) | 4.73(77) |
| Yale, BC | 593(17) | 5.80(62) | 595(12) | 6.40(95) | 601(8) | 6.38(95) | 601(8) | 6.36(96) |
| Penfold Cr. | 604(67) | 4.58(1.09) | 598(65) | 4.80(1.52) | 607(32) | 4.66(99) | 607(31) | 4.61(94) |
| Lepontine Alps | 605(74) | 6.18(1.49) | 610(66) | 7.25(1.85) | 607(40) | 7.11(1.57) | 607(39) | 6.93(1.58) |

*Note:* Complete *T* and *P* results are given in Table 3 (Footnote 1).
* See Table 2 for complete localities and references.

rich fluid, lower *P* in a few cases, and experimental error will lower the minimum *T* by up to 50 °C, but Zn and Li in staurolite will raise it slightly. Thus a *T* of about 550 °C appears reasonable for the first appearance of the Al-silicate–biotite–garnet–muscovite assemblage of these specimens. Kerrick (1972) showed that reaction 4 proceeds in vapor-absent conditions, producing melt, at *T* of 650–675 °C. Experimental error and additional components such as Ca could increase this figure to about 700 °C. Thus it appears reasonable that the likely range of *T* for the assemblage of the muscovite-bearing specimens is 550 to 700 °C, consistent with the eight new calibrations presented here (Table 4, Fig. 2c–2d).

In summary, the eight new calibrations represent an improvement over the previous two calibrations. The *T* values calculated from the average garnet model are a slight improvement over *T* values calculated from the individual garnet models (Holdaway 2000). I tentatively adopt the Fuhrman and Lindsley (1988) plagioclase model (for reasons given in the next section), the average garnet model, and *T* values calculated from the average garnet model (GASPAF, Table 4, Fig. 2c) as the preferred model.

## PLAGIOCLASE ACTIVITY MODEL

Careful scrutiny of Figure 2c–d and Table 4 shows that the Elkins and Grove (1990) plagioclase model (GASPAE) appears to give slightly better results than the Fuhrman and Lindsley (1988) model (GASPAF). However, the differences are small and involve only a few samples. The Fuhrman and Lindsley (1988) model is based on the experimental data of Seck (1971a, 1971b) for which compositions were determined by X-ray *d* spacings and geometric constraints. The data of Seck were fit to an Al-avoidance plagioclase model for ideal configurational entropy that was originally proposed by Kerrick and Darken (1975). Elkins and Grove (1990) measured compositions of experimental product feldspars with the electron microprobe. They were unable to fit their data to the Al-avoidance model and instead used a simple one-site (local charge balance) model for plagioclase.

Figure 3 is a scatter plot of $\Delta P$ ($P_{GASPAF} - P_{GASPAE}$) vs. percent anorthite in plagioclase for all 76 calibration samples plus the 59 Alpine samples discussed below. As a result of adjusting the end-member curve to fit the natural data to the K-S curve, the two calibrations agree to within less than about 0.2 kbar over the range $An_{22}$ to $An_{48}$, which includes most of the samples used for calibration. However, at anorthite contents less than $An_{22}$ and greater than $An_{48}$, the two calibrations disagree by about 0.2 to 0.6 kbar, depending on plagioclase composition. These few extreme samples could be used to determine the best plagioclase model. If other factors are equal, these extreme compositions should produce a reduced range of *P* for multiple samples within an individual locality for the best model.

Table 5 gives values of σ for each of the 11 localities included in this calibration. Most of the σ values are similar or

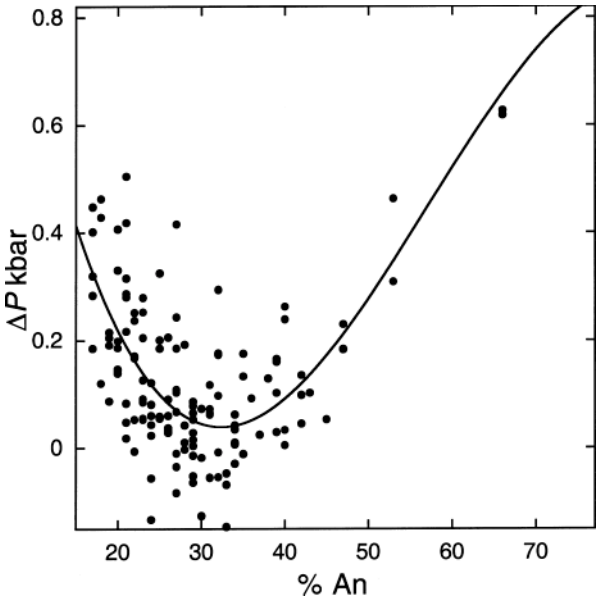


**FIGURE 3.** Scatter plot of $P_{GASPAF} - P_{GASPAE}$ ($\Delta P$) vs. % An for 76 samples from 11 localities and 59 samples from the Lepontine Alps (Table 2). The rough agreement between the two calibrations (GASPAF and GASPAE) over the range $An_{22}$ to $An_{48}$ results from the method of determining the calibration. (See text for further explanation.)

smaller for the Elkins and Grove (1990) model than for the Fuhrman and Lindsley (1988) model. To quantify this effect, weighted average σ (sum of σ of each locality times its number of samples, the total divided by 76) was calculated for each model. This weighted average σ for the Elkins and Grove model is 0.694 kbar vs. 0.709 kbar for Fuhrman and Lindsley. Weighted average σ for the Elkins and Grove model is thus 97.9% as much as for the Fuhrman and Lindsley model. However, this effect may be explained by the fact that the average value of $P_o - P$ ($P$ correction from the end-member curve to the actual $P$ resulting from dilution of grossular and anorthite) differs between the two plagioclase models. If the two plagioclase models were equivalent in quality, weighted average σ would be reduced by the same proportion as average $P_o - P$ is reduced, because the plagioclase model is the only difference between the two sets of calculations. Reduction of average $P_o - P$ simply telescopes the calculated results. The end-member curve for GASPAE is steeper than that for GASPAF, and passes through 11.613 kbar at the average $T$ of 606.6 °C vs. 12.276 kbar at the average $T$ of 606.9 °C for GASPAF. Average $P$ values for the 76 samples are 5.251 kbar for GASPAE and 5.351 kbar for GASPAF. Thus average $P_o - P$ is 6.362 kbar for GASPAE and 6.925 kbar for GASPAF, or 92% as large. If the two plagioclase models were equivalent in quality, the smaller $P_o - P$ should shrink weighted average σ by 8% instead of only 2.1%. Even though σ values for several of the localities are a little smaller and the fit with the kyanite curve appears slightly better, the effect is simply the result of the smaller $P_o - P$ for the GASPAE model, and the effect is actually less than it should be, indicating that GASPAF is the better model. This result will be supported below with the treatment of the Lepontine Alps data.

The four models that involve the Fuhrman and Lindsley (1988) plagioclase activity model have additional advantages over the Elkins and Grove (1990) plagioclase activity model: (1) The $H_{grs}$ and $S_{grs}$ values for Fuhrman and Lindsley plagioclase (Table 4) are closer to those of Berman (1988, revised 1992); and (2) three of the $H_{grs}$ and $S_{grs}$ values for Elkins and Grove plagioclase give GASP end-member curves that violate two or more extended end-member constraints (Figs. 1c and 1d). As previously stated, my only reason for preferring the average model (GASPAF) over the other garnet models is that it provides a better geothermometer (Holdaway 2000).

## AN INDEPENDENT TEST

A suite of pelitic schists from the Swiss Lepontine Alps (Engi et al. 1995, Todd and Engi 1997) was chosen for independent verification of the geobarometer. For these, the peak-$T$ garnet and plagioclase compositions selected by the authors were used. In all, 63 samples met the constraints given above. However, 4 of these samples were rejected because calculated $P$ plots in the wrong field by 1 to 3 kbar for all eight calibrations. These samples are discussed below. The Alpine specimens range to significantly higher An (17-74) and Grs (3-23) content than specimens from the 11 localities used for calibration combined (Table 2). Apparently, the Alpine pelitic schists originally contained a significantly larger range of calcite (and possibly ankerite) component than most other pelitic metamorphic rocks.

Most of the Alpine samples plot in the appropriate phase fields (Figs. 4a–d, Table 6). Note that the $P$ and $T$ scales of Figure 2 and Figure 4 are the same, but for Figure 4 the range of $P$ is shifted to higher values. The problems with the Hodges and Spear (1982) calibration (Fig. 4a) are more obvious than with the calibration set because their simple plagioclase activity model does not work well at high An contents and leads to several kyanite-bearing rocks plotting far into the sillimanite field. The K-S boundary falls closer to the middle of the overlap range for the other nine calibrations (Table 6, Figs. 4b–d). The overlap range for the Alpine samples is almost twice as large as for the other 11 localities, and a greater percentage of samples lie in the wrong field by more than 0.15 kbar. In addition, a larger percentage of the Alpine samples was rejected

**TABLE 6.** Comparison of two previous GASP calibrations and eight present calibrations for the alpine samples

| Model | Overlap Range (kbar) | Midpoint Relative to K-S* (kbar) | No. in Violation > 0.15 kbar |
|---|---|---|---|
| GASPHS | 3.04 | –0.99 | 15 |
| GASPB92 | 1.69 | –0.13 | 6 |
| GASPGF | 1.54 | –0.15 | 7 |
| GASPMF | 1.46 | –0.14 | 7 |
| GASPBF | 1.56 | –0.12 | 7 |
| GASPAF | 1.52 | –0.14 | 7 |
| GASPGE | 1.64 | –0.28 | 10 |
| GASPME | 1.50 | –0.23 | 10 |
| GASPBE | 1.68 | –0.21 | 10 |
| GASPAE | 1.62 | –0.25 | 10 |

*Notes:* Data based on 59 natural samples from Engi et al. 1995 and Todd and Engi 1997, Table 3 (Footnote 1), and Figures 3a–d. Models and explanation are given in text. See Table 4 for GASP end-member data for each model.
* Midpoint of overlap range relative to the kyanite-sillimanite boundary.

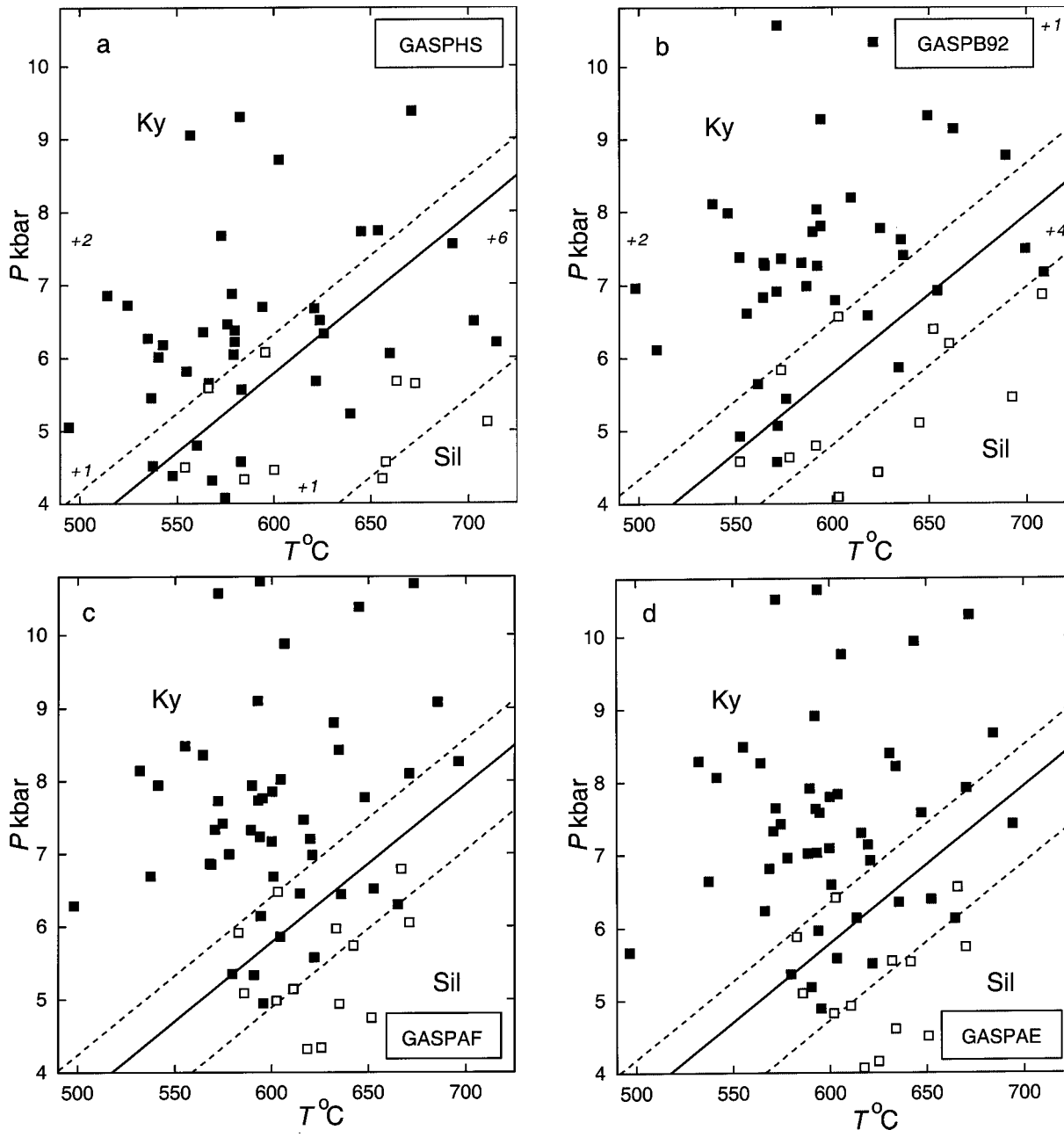


**FIGURE 4.** Calculated *P* and *T* for 59 samples from the Lepontine Alps (4 additional samples were rejected as explained in text). For ease of comparison, all four plots occupy the same limited *P-T* field, which ranges to higher values of *P* than the plots of Figure 2. Other information is as given in the caption to Figure 2. For (**a**) *P-T* points outside the field include K = 6.24, 488; 6.26, 475; 3.24, 428; 8.02, 729; 9.09, 764; 6.70, 758; 10.33, 732; and S = 3.91, 623; 6.04, 726; 7.19, 742. [The lower field of overlap for **a** is bounded by the Kyanite-bearing *P-T* point at 6.70, 758). For (**b**) *P-T* points outside the field include K = 5.24, 444; 7.05, 487; 9.30,726; 10.73, 758; 9.05, 739; 12.36, 739; and S = 8.02, 734.]

than for the calibration set. The Fuhrman and Lindsley (1988) plagioclase model appears to give slightly better results than the Elkins and Grove (1990) plagioclase model (Table 6). Of greater significance is the fact that σ for both sets is essentially the same, 1.574 kbar for GASPAF and 1.575 for GASPAE (Table 5). This similar range of *P* values can also be seen by inspection of Figure 4c and 4d. If the Elkins and Grove model were the better model, σ for GASPAE should be less than 92% as large (see above) as for GASPAF. The results from the wider range of plagioclase compositions for the Alpine samples thus support the choice of Fuhrman and Lindsley (1988) as the better plagioclase activity model.

## ANALYSIS OF ERROR

A rigorous analysis of error for these calibrations is not possible because of the method of calibration and the various sources of analytical data used. However, it is possible to estimate rough values of absolute and relative 2σ error by making some reasonable approximations. For purposes of this analysis, error sources are grouped into the following three subequal independent categories: (1) error from misfit to the K-S boundary that must have resulted from analytical, geological, activity model, and reaction 1 $\Delta H$, $\Delta S$, and $\Delta V$ error; (2) error in the determination of the K-S boundary; (3) the effect of $T$ error on $P$ error. Temperature error is estimated to be ±25 °C absolute, ±15 °C relative by Holdaway (2000). Much of the error in activity models is compensated for by the end-member calibration (various values of $H_{Grs}$ and $S_{Grs}$, Table 4) as a result of the method of calibration. The absolute and relative errors discussed below are approximate values that can be achieved if careful procedures are used and reasonable steps are taken to avoid data that could produce outliers, as discussed below. The estimates apply to the recommended calibration using the average garnet model, the corresponding $T$ model, and the Fuhrman and Lindsley (1988) plagioclase model (GASPAF). Errors for the other calibrations are expected to be slightly larger.

## ABSOLUTE ERROR

This is the maximum estimated error in $P$. The three parts are: (1) maximum misfit error of 0.43 kbar is between 1σ and 2σ, estimated to be 1.5σ (2σ = ±0.57 kbar); (2) error in the K-S curve, is estimated to be ±0.40 kbar; (3) temperature-based $P$ error is 0.020 × 25 = ±0.50 kbar for the kyanite field, 0.017 × 25 = ±0.43 kbar for the sillimanite field, based on average GASP equilibrium slopes in the kyanite and sillimanite fields, respectively. The *rms* error is thus ±0.86 kbar in the kyanite field and ±0.82 kbar in the sillimanite field.

## RELATIVE ERROR

This is the estimated error that can be expected when comparing several pressure determinations using the present recommended calibrations for $T$ and $P$. The above-determined error is reduced by eliminating the K-S curve error and reducing the $T$ error to ±15 °C. For the kyanite field the error is ±0.64 kbar, and for the sillimanite field the error is ±0.62 kbar.

## ANALYSIS OF OUTLIERS

A significant fact of life with the GASP geobarometer is the existence of outliers. This is especially true when using the results of other workers in a study such as this one, where procedures varied between workers. The above error estimates are only realistic if ways can be found to avoid outliers such as those that were rejected for this study. The three samples from the calibration localities and four from the Lepontine Alps that were rejected could only be identified because the samples crystallized near the K-S boundary and the error was in the direction of the boundary. Other samples may have similar error but not be so judiciously placed in the $P$-$T$ field. At the same time, most samples must not have such large errors, or the orderly pattern seen in Figures 2 and 4 would not have occurred. Table 7 lists all samples (referred to as misfit samples) in both data sets that violate the K-S boundary by more than 0.15 kbar, including these rejected samples.

In all but one case, the misfit samples show similar degree of misfit regardless of which of the eight calibrations is used. This result indicates that much of the error involved in these samples is geological and/or analytical, and the other error

**TABLE 7.** Misfit samples, including rejected outliers, that plot in the wrong Al silicate field by more than 0.15 kbar, ranked in order of decreasing degree of misfit according to the average garnet and Fuhrman and Lindsley (1988) plagioclase (GASPAF) calibration

| Sample Number | Locality | Reference | Misfit† (kbar) | Misfit Range (kbar)‡ | | | | % Grs | % An |
|---|---|---|---|---|---|---|---|---|---|
| | | | | FUHR | | ELKI | | | |
| | | | | Max | Min | Max | Min | | |
| Eleven Localities, used for Calibration | | | | | | | | | |
| 140817R* | Grampian High. | McLellan (1985) | 3.59 | 3.61 | 3.58 | 3.44 | 3.36 | 15.3 | 28 |
| 140900R* | Grampian High. | McLellan (1985) | 1.90 | 1.92 | 1.88 | 1.79 | 1.72 | 9.4 | 26 |
| 140980R* | Grampian High. | McLellan (1985) | 1.29 | 1.33 | 1.26 | 1.13 | 1.04 | 7.1 | 23 |
| 2-376* | Azure Lake | Pigage (1982) | 0.43 | 0.51 | 0.37 | 0.52 | 0.34 | 7.3 | 28 |
| 121 | Azure Lake | Pigage (1982) | –0.42 | –0.48 | –0.33 | –0.47 | –0.29 | 7.1 | 34 |
| HV10H | Hunt Valley Mall | Lang (1991) | –0.30 | –0.34 | –0.28 | –0.36 | –0.28 | 6.2 | 29 |
| 83131R* | Grampian High. | McLellan (1985) | 0.23 | 0.28 | 0.16 | 0.00 | 0.00 | 5.3 | 21 |
| Lepontine Alps, used for Verification | | | | | | | | | |
| MA9353 | Lepontine Alps | Engi et al. (1995) | –2.79 | –2.95 | –2.71 | –3.16 | –2.91 | 3.1 | 28 |
| KL437* | Lepontine Alps | Koch (1982) | 1.90 | 1.95 | 1.83 | 1.55 | 1.48 | 7.3 | 21 |
| MAG193 | Lepontine Alps | Engi et al. (1995) | –1.33 | –1.61 | –1.16 | –1.81 | –1.36 | 5.2 | 34 |
| AI518* | Lepontine Alps | Irouschek (1983) | 1.20 | 1.24 | 1.23 | 1.14 | 1.09 | 8.9 | 29 |
| MAG352 | Lepontine Alps | Engi et al. (1995) | –0.93 | –0.92 | –0.87 | –1.10 | –1.03 | 6.1 | 32 |
| MAG096 | Lepontine Alps | Engi et al. (1995) | –0.75 | –0.77 | –0.71 | –0.83 | –0.76 | 4.6 | 25 |
| MA9364 | Lepontine Alps | Engi et al. (1995) | –0.69 | –0.70 | –0.65 | –0.78 | –0.71 | 6.1 | 31 |
| MA9418 | Lepontine Alps | Todd and Engi (1997) | 0.63 | 0.67 | 0.59 | 0.63 | 0.52 | 7.2 | 27 |
| KL185 | Lepontine Alps | Koch (1982) | 0.50 | 0.56 | 0.43 | 0.55 | 0.37 | 6.0 | 24 |
| MAG540 | Lepontine Alps | Engi et al. (1995) | –0.40 | –0.45 | –0.37 | –0.56 | –0.51 | 7.5 | 35 |
| DS08 | Lepontine Alps | Engi et al. (1995) | –0.25 | –0.29 | –0.22 | –0.44 | –0.36 | 4.0 | 20 |

* Misfit samples which contain both Al silicates but plot in the kyanite field.
† Positive values – sillimanite in kyanite field, negative values – kyanite in sillimanite field, 0.00 – plots in the correct field.
‡ Range of misfit for Fuhrman and Lindsley (1988) – FUHR, and Elkins and Grove (1990) – ELKI plagioclase activity model, using all four garnet and $T$ models of this report.

sources (activity models, reaction 1 $\Delta H$, $\Delta S$ and $\Delta V$) are smaller and, to a certain extent, compensate for each other. It is more difficult to distinguish between the two possibilities of analytical and geological error. Samples that should show the largest analytical error are those with lowest Grs and An contents because of the increased relative error that results from low analytical values (Todd 1998). Low Grs and An samples are not common in this group, although one rejected Alpine sample has 3.1% Grs, only slightly over the threshold value. Table 8 shows that for the 11 calibration localities, the misfit samples are compositionally no different from the set as a whole. The Alpine suite shows slight lowering of the average of the An and Grs content of the misfit samples, but the effect is small. Also, there is no trend of decreasing Grs and/or An with increasing misfit as one would expect if analytical error were the main source of error for these samples. The fact that the Grampian Highlands and the Lepontine Alps are the worst offenders and also show the two highest $\sigma$ values in $P$ (Table 5) suggests that geological error is a major factor in the error of the misfit samples. The larger range of $P$ for these regions could have produced larger ranges of $P$ for individual samples during their crystallization history. This in turn is likely to have produced larger $P$ error. The analytical and geological error can be reduced by following the procedures suggested in the next section.

A specific type of geologic error is that resulting from the failure of the assumption that sillimanite is the high-$T$ mineral when both Al-silicates occur in the same sample. This kind of error could occur in some samples that contain both Al-silicates and plot in the kyanite field. Such specimens are identified with an asterisk in Table 7. In most cases, the samples were identified by the authors as reaching sillimanite-grade as the peak-$T$ condition. For any samples in which kyanite actually is the high-$T$ mineral and both Al-silicates are present, this becomes an explanation for the misfit, and also a possible shortcoming of the procedure used to distinguish which Al-silicate was the high-$T$ form when both were present. Fortunately, such samples appear to be in the minority.

Finally, Todd and Engi (1997, Fig. 13) point out that a few samples that contain kyanite and no sillimanite plot in the sillimanite $P$-$T$ field using their geobarometry.

## Suggestions for use of the GASP geobarometer

The main emphasis in selection of samples and locations within a sample for analysis must be to eliminate the possibility of samples such as those that had to be rejected for this study. The procedures used here (or, possibly, more restrictive limits, Todd 1998) are recommended for rejection of low-An (<17%) and low-Grs (<3%) samples and for determination of the peak-$T$ Al silicate.

To achieve errors not larger than those quoted above, it is necessary to minimize analytical and geological error. Analytical error can be reduced by maintaining good calibration and instrument stability and, if there is any chance of short-term spectrometer drift, analyzing Fe and Mg in garnet and biotite adjacent in time and, as much as possible, Ca in garnet and plagioclase adjacent in time. Some suggestions for reduction of geological error include: (1) analyze more than one garnet in a sample with surrounding biotite and plagioclase for each, where possible; analyze two samples from the same outcrop; and analyze multiple samples from a region to show trends of $P$ and $T$, such that spurious samples can be identified from disagreement with the trends of the remaining samples; (2) analyzed plagioclase and biotite should be located close to the analyzed garnet; (3) perhaps most important, the same part of the rock's history, preferably peak-$T$, should be represented by the analyzed zone of the garnet as the analyzed zone of the plagioclase, and this part of the history should be represented by the correct Al-silicate, identified by textural analysis for samples containing both Al-silicates. Determination of the correct peak-$T$ compositions and assemblage is very difficult to do well in rocks that had complicated $P$-$T$ histories or large $P$ variations during crystallization.

**TABLE 8.** Comparison of average and $\sigma$, (in parentheses) of grossular and anorthite percentages of complete data sets with average and $\sigma$ of the misfit samples, including rejected outliers, that plot in the wrong Al silicate field by more than 0.15 kbar (Table 7)

| Sample set | n | % Grs | % An |
|---|---|---|---|
| Complete set, 11 localities | 79 | 6.3(2.5) | 28(7) |
| Misfit samples, 11 localities | 7 | 8.2(3.4) | 27(4) |
| Complete set, Alps | 63 | 9.9(5.6) | 30(12) |
| Misfit samples, Alps | 11 | 6.0(1.7) | 28(5) |

## Conclusion

Based on the above results, some important conclusions can be drawn. (1) Thermodynamic databases, end-member calibration for GASP, and garnet and plagioclase activity models are not sufficiently well known for the end-member curve and the garnet and plagioclase activity models to be used independently. Any given combination of garnet and plagioclase models must be reconciled with the end-member curve to produce a useful GASP calibration. (2) Fitting the GASP end-member curve to the K-S curve provides a self-consistent system that minimizes Al-silicate misfit and error. (3) Good quality determination of $T$ is paramount for good estimates of $P$ with GASP. (4) Considering the above constraints, the best overall calibration of GASP appears to be the one based on the garnet-biotite geothermometer that uses the average garnet activity model, the average garnet activity model for GASP, and the Fuhrman and Lindsley (1988) plagioclase activity model (GASPAF). All eight models calibrated for this report are available in a set of three PC computer programs for use on a DOS platform ($P$, $T$, and $P$-$T$ intersection), which may be obtained by writing the author.

## Acknowledgments

I thank Biswajit Mukhopadhyay for writing original versions of some of the computer programs and Clifford Todd (Univ. Hawaii) for providing analyses and data for the Alpine specimens. Bob Tracy, Kip Hodges, and Rick Ryerson provided constructive reviews.

## References cited

Berman, R.G. (1988) Internally consistent thermodynamic data for stoichiometric minerals in the system $Na_2O$-$K_2O$-CaO-MgO-FeO-$Fe_2O_3$-$Al_2O_3$-$SiO_2$-$TiO_2$-$H_2O$-$CO_2$. Journal of Petrology, 29, 445–522.

———(1990) Mixing properties of Ca-Mg-Fe-Mn garnets. American Mineralogist, 75, 328–344.

Berman, R.G. and Aranovich, L.Y. (1996) Optimized standard state and solution

properties of minerals. I. Model calibration for olivine, orthopyroxene, cordierite, garnet, and ilmenite in the system FeO-MgO-CaO-$Al_2O_3$-$TiO_2$-$SiO_2$. Contributions to Mineralogy and Petrology, 126, 1–24.
Elkins, L.T. and Grove, T.L. (1990) Ternary feldspar experiments and thermodynamic models. American Mineralogist, 75, 544–559.
Engi, M., Todd, C.S., and Schmatz, D.R. (1995) Tertiary metamorphic conditions in the eastern Lepontine Alps. Schweizerische Mineralogische und Petrographische Mitteilungen, 75, 347–369.
Ferry, J.M. (1980) A comparative study of geothermometers and geobarometers in pelitic schists from south-central Maine. American Mineralogist, 65, 720–732.
Fletcher, C.J.N. and Greenwood, H.J. (1979) Metamorphism and structure of Penfold Creek area near Quesnal Lake, British Columbia. Journal of Petrology, 20, 743–794.
Fuhrman, M.L. and Lindsley, D.H. (1988) Ternary-feldspar modeling and thermometry. American Mineralogist, 73, 201–215.
Ganguly, J., Cheng, W., and Tirone, M. (1996) Thermodynamics of aluminosilicate garnet solid solution: new experimental data, an optimized model, and thermometric applications. Contributions to Mineralogy and Petrology, 126, 137–151.
Gasparik, T. (1984) Experimental study of the subsolidus phase relations and mixing properties of pyroxene in the system CaO-$Al_2O_3$-$SiO_2$. Geochimica et Cosmochimica Acta, 48, 2537–2545.
Ghent, E.D. (1976) Plagioclase-garnet-$Al_2SiO_5$-quartz: a potential geothermometer-geobarometer. American Mineralogist, 61, 710–714.
Goldsmith, J.R. (1980) Melting and breakdown reactions of anorthite at high pressures and temperatures. American Mineralogist, 65, 272–284.
Hariya, Y. and Kennedy, G.C. (1968) Equilibrium study of anorthite under high temperature and high pressure. American Journal of Science, 266, 193–203.
Hays, J.F. (1966) Lime-alumina-silica. Carnegie Institution of Washington Yearbook, 65, 234–239.
Hodges, K.V. and McKenna, L.W. (1987) Realistic propagation of uncertainties in geologic thermobarometry. American Mineralogist, 72, 671–680.
Hodges, K.V. and Spear, F.S. (1982) Geothermometry, geobarometry and the $Al_2SiO_5$ triple point at Mt. Moosilauke, New Hampshire. American Mineralogist, 67, 1118–1134.
Holdaway, M.J. (2000) Application of new experimental and garnet Margules data to the garnet-biotite geothermometer. American Mineralogist, 85, 881–892.
Holdaway, M.J. and Mukhopadhyay, B. (1993) A reevaluation of the stability relations of andalusite; Thermochemical data and phase diagram for the aluminum silicates. American Mineralogist, 78, 681–693.
Holdaway, M.J., Guidotti, C.V., Novak, J.M., and Henry, W.E. (1982) Polymetamorphism in medium- to high-grade pelitic metamorphic rocks, west-central Maine. Geological Society of America Bulletin, 93, 572–584.
Holdaway, M.J., Dutrow, B.L., and Hinton, R.W. (1988) Devonian and Carboniferous metamorphism in west-central Maine: the muscovite-almandine geobarometer and the staurolite problem revisited. American Mineralogist, 73, 20–47.
Holdaway, M.J., Mukhopadhyay, B., Dyar, M.D., Guidotti, C.V., and Dutrow, B.L. (1997) Garnet-biotite geothermometry revised: new Margules parameters and a natural specimen data set from Maine. American Mineralogist, 82, 582–595.
Irouschek, A. (1983) Mineralogie und Petrographie von Metapeliten der Simano-Decke unter besonderer Berücksichtigung cordieritführender Gesteine zwischen Alpe Sponda und Biasca. Ph.D. Thesis, Universität Basel, Switzerland.
Kerrick, D.M. (1972) Experimental determination of muscovite + quartz stability with $P_{H_2O} < P_{total}$. American Journal of Science, 272, 946–958.
Kerrick, D.M. and Darken, L.S. (1975) Statistical thermodynamic models for ideal oxide and silicate solid solutions, with application to plagioclase. Geochimica et Cosmochimica Acta, 39, 1431–1442.
Koziol, A.M. and Newton, R.C. (1988) Redetermination of the anorthite breakdown reaction and improvement of the plagioclase-garnet-$Al_2SiO_5$-quartz geobarometer. American Mineralogist, 73, 216–223.
Koch, E. (1982) Mineralogie und plurifazielle Metamorphose der Pelite in der Adula-Decke (Zentralalpen). Ph.D. Thesis, Universität Basel, Switzerland.
Lang, H.M. (1991) Quantitative interpretation of within-outcrop variation in metamorphic assemblages in staurolite-kyanite-grade metapelites, Baltimore, Maryland. Canadian Mineralogist, 29, 655–671.
Lang, H.M. and Rice, J.M. (1985a) Regression modeling of metamorphic reactions in metapelites, Snow Peak, northern Idaho. Journal of Petrology, 26, 857–887.
———(1985b) Geothermometry, geobarometry and *T-X*(Fe-Mg) relations in metapelites, Snow Peak, northern Idaho. Journal of Petrology, 26, 889–924.
McKenna, L.W. and Hodges, K.V. (1988) Accuracy versus precision in locating reaction boundaries: Implications for the garnet-plagioclase-aluminum silicate-quartz geobarometer. American Mineralogist, 73, 1205–1208.
McLellan, E. (1985) Metamorphic reactions in the kyanite and sillimanite zones of the Barrovian type area. Journal of Petrology, 26, 789–818.
McMullin, D.W.A., Berman, R.G., and Greenwood, H.J. (1991) Calibration of the SGAM thermobarometer for pelitic rocks using data from phase-equilibrium experiments and natural assemblages. Canadian Mineralogist, 29, 889–908.
Mukhopadhyay, B., Basu, S., and Holdaway, M.J. (1993) A discussion of Margules-type formulations for multicomponent solutions with a generalized approach. Geochimica et Cosmochimica Acta, 57, 277–283.
Mukhopadhyay, B., Holdaway, M.J., and Koziol, A.M. (1997) A statistical model of thermodynamic mixing properties of Ca-Mg-$Fe^{2+}$ garnets. American Mineralogist, 82, 165–181.
Novak, J.M. and Holdaway, M.J. (1981) Metamorphic petrology, mineral equilibria, and polymetamorphism in the Augusta quadrangle, south-central Maine. American Mineralogist, 66, 51–69.
Pigage, L.C. (1976) Metamorphism of the Settler Schist, southwest of Yale, British Columbia. Canadian Journal of Earth Science, 13, 405–421.
———(1982) Linear regression analysis of sillimanite-forming reactions at Azure Lake, British Columbia. Canadian Mineralogist, 20, 349–378.
Seck, H.A. (1971a) Koexistierende Alkalifeldspät und Plagioklase im System $NaAlSi_3O_8$-$KAlSi_3O_8$-$CaAl_2Si_2O_8$-$H_2O$ bei Temperaturen von 650 °C bis 900 °C. Neues Jahrbuch für Mineralogie Abhandlungen, 115, 315–345.
———(1971b) Der Einfluss des Drucks auf die Zusammensetzung koexistierender Alkalifeldspäte und Plagioklase. Contributions to Mineralogy and Petrology, 31, 67–86.
Spear, F.S. (1993) Metamorphic phase equilibria and pressure-temperature-time paths. Mineralogical Society of America Monograph, 799 p. Mineralogical Society of America, Washington, D.C.
Spear, F.S., Kohn, M.J., and Paetzold, S. (1995) Petrology of the regional sillimanite zone, west-central New Hampshire, U.S.A., with implications for the development of inverted isograds. American Mineralogist, 80, 361–376.
Todd, C.S. (1998) Limits on the precision of geothermometry at low grossular and anorthite content. American Mineralogist, 83, 1161–1167.
Todd, C.S. and Engi, M. (1997) Metamorphic field gradients in the Central Alps. Journal of Metamorphic Geology, 15, 513–530.
Tracy, R.J. (1975) High grade metamorphic reactions and partial melting in pelitic schist, Quabbin Reservoir area, Massachusetts. Ph.D. Thesis. University of Massachusetts, Amherst, Massachusetts, 127 p.

MANUSCRIPT RECEIVED AUGUST 25, 2000
MANUSCRIPT ACCEPTED MAY 29, 2001
MANUSCRIPT HANDLED BY RICK RYERSON

**NOTE ADDED IN PRESS:** I recently discovered an error in data entry. For garnet, the stoichiometry must always be based on 12 O atoms, 8 cations, or 3 divalent cations, and for some, I had used a basis of double or one third of those values. An incorrect garnet basis changes the percentage of $Fe^{3+}$ in the Al sites, according to the method of calculation. Correcting the data entries results in *P* values lower by about 0.05 kbar for 2 Hunt Valley Mall samples, 6 Augusta, Maine samples, and the Alpine samples; and *P* values about 0.10 kbar higher for 6 Penfold Creek samples. The correct values are given on Table 3 (for deposit). Neither the calibrations nor the results were affected by this error.